

1 **The impact of BNT162b2 mRNA vaccine on adaptive and** 2 **innate immune responses**

3 Short title: BNT162b2 effect on adaptive and innate immune responses

4

5 Konstantin Föhse^{1,2¶}, Büsra Geckin^{1,2¶}, Martijn Zoodma^{3,4¶}, Gizem Kilic^{1,2}, Zhaoli Liu^{3,4}, Rutger J.
6 Röring^{1,2}, Gijs J. Overheul⁵, Josephine S. van de Maat^{1,2}, Ozlem Bulut^{1,2}, Jacobien J. Hoogerwerf^{1,2},
7 Jaap ten Oever^{1,2}, Elles Simonetti⁶, Heiner Schaal⁷, Ortwin Adams⁷, Lisa Müller⁷, Philipp Niklas
8 Ostermann⁷, Frank L. van de Veerdonk^{1,2}, Leo A.B. Joosten^{1,2,6}, Bart L. Haagmans⁹, Reinout van
9 Crevel^{1,2}, Ronald P. van Rij⁵, Corine GeurtsvanKessel⁹, Marien I. de Jonge⁶, Yang Li^{3,4&}, Jorge
10 Domínguez-Andrés^{1,2&}, Mihai G. Netea^{1,2&*}

11

12 ¹Department of Internal Medicine and Radboud Center for Infectious Diseases, Radboud University
13 Medical Center, Nijmegen, The Netherlands

14 ²Radboud Institute for Molecular Life Sciences, Radboud University Medical Center, Nijmegen, The
15 Netherlands

16 ³Department of Computational Biology for Individualised Infection Medicine, Centre for
17 Individualised Infection Medicine (CiiM), a joint venture between the Helmholtz-Centre for Infection
18 Research (HZI) and the Hannover Medical School (MHH), Hannover, Germany

19 ⁴TWINCORE, a joint venture between the Helmholtz-Centre for Infection Research (HZI) and the
20 Hannover Medical School (MHH), Hannover, Germany

21 ⁵Department of Medical Microbiology, Radboud University Medical Center, Nijmegen, The
22 Netherlands

23 ⁶Department of Laboratory Medicine, Laboratory of Medical Immunology, Radboud Center for
24 Infectious Diseases, Radboudumc, Nijmegen, The Netherlands

25 ⁷Institute of Virology, Medical Faculty, University Hospital Düsseldorf, Heinrich-Heine-Universität,
26 Düsseldorf, Germany

27 ⁸Department of Medical Genetics, Iuliu Hatieganu University of Medicine and Pharmacy, Cluj-
28 Napoca, Romania

29 ⁹Department of Viroscience, Erasmus MC, Rotterdam, The Netherlands

30

31 * Corresponding author

32 E-mail: mihai.netea@radboudumc.nl

33

34 ¶These authors contributed equally to this work.

35 &These authors also contributed equally to this work.

NOTE: This preprint reports new research that has not been certified by peer review and should not be used to guide clinical practice.

36 **Abstract**

37 The mRNA-based BNT162b2 protects against severe disease and mortality caused by SARS-
38 CoV-2 through induction of specific antibody and T-cell responses. Much less is known about
39 its broad effects on immune responses against other pathogens. In the present study, we
40 investigated the specific adaptive immune responses induced by BNT162b2 vaccination
41 against various SARS-CoV-2 variants, as well as its effects on the responsiveness of human
42 immune cells upon stimulation with heterologous viral, bacterial, and fungal pathogens.
43 BNT162b2 vaccination induced effective humoral and cellular immunity against SARS-CoV-
44 2 that started to wane after six months. We also observed long-term transcriptional changes in
45 immune cells after vaccination, as assessed by RNA sequencing. Additionally, vaccination
46 with BNT162b2 modulated innate immune responses as measured by the production of
47 inflammatory cytokines when stimulated with various microbial stimuli other than SARS-
48 CoV-2, including higher IL-1/IL-6 release and decreased production of IFN- α . Altogether,
49 these data expand our knowledge regarding the overall immunological effects of this new class
50 of vaccines and underline the need of additional studies to elucidate their effects on both innate
51 and adaptive immune responses.

52

53 **Introduction**

54 The mRNA vaccine developed by BioNTech and Pfizer (BNT162b2) was approved for
55 emergency use due to the protection induced against SARS-CoV-2 infection. It took less than
56 eight months after trials started to achieve this landmark. This vaccine is based on a lipid
57 nanoparticle-formulated, nucleoside-modified mRNA that encodes a prefusion stabilized form
58 of the spike (S)-protein derived from the SARS-CoV-2 strain isolated at the beginning of the

59 outbreak in Wuhan, China [1]. Multiple phase-3 trials have demonstrated that BNT162b2
60 elicits broad humoral and cellular-specific responses, providing protection against COVID-19
61 [1–3].

62 While the induction of specific immunity against SARS-CoV-2 has been intensively studied,
63 much less is known about the effects of this new class of mRNA vaccines against heterologous
64 pathogens. The lipid nanoparticle (LNP) component of those vaccines was reported to induce
65 strong pro-inflammatory responses [4], and recent studies have shown that BNT162b2 can also
66 induce long-term transcriptional changes in myeloid cells [5,6]. This suggests that the response
67 of immune cells against various microorganisms other than SARS-CoV-2 could also change
68 after BNT162b2 vaccination. Other vaccines, such as Bacillus Calmette-Guérin (BCG) or
69 influenza A virus vaccines, but also the novel adenoviral-based COVID-19 vaccines, have been
70 shown to induce long-term functional changes in innate immune cells, also called *trained*
71 *immunity*, that subsequently results in heterologous protective effects [7–9]. There is much less
72 data available on the functional effects of BNT162b2 vaccination on immune responses
73 towards other pathogens than SARS-CoV-2.

74 With this in mind, we investigated the effects of BNT162b2 vaccination on both the specific
75 adaptive immune responses and the responsiveness of human immune cells upon stimulation
76 with heterologous pathogens. These experiments confirmed that BNT162b2 vaccination of
77 healthy individuals induced effective humoral and cellular immunity against SARS-CoV-2,
78 which started to wane after six months, especially against new variants. Interestingly, RNA
79 sequencing revealed long-term changes in the transcriptional programs of immune cells after
80 administration of the BNT162b2 vaccine, and vaccination also modulated the production of
81 inflammatory cytokines upon stimulation with viral, bacterial, and fungal stimuli. The
82 synthesis and release of myeloid-derived cytokines from the IL-1/IL-6 pathway tended to be

83 higher six months after the first dose of BNT162b2. In contrast, the production of IFN- α after
84 stimulation with SARS-CoV-2, TLR3 ligand poly I:C, and TLR7/8 ligand R848 decreased after
85 vaccination. Altogether, we observed that administration of the BNT162b2 vaccine modulated
86 innate immune responses up to one year after the initial vaccination. These data contribute to
87 our understanding of the broad immunological effects of mRNA vaccines and underline the
88 importance of performing additional studies to elucidate their full potential effects on innate
89 and adaptive immune responses.

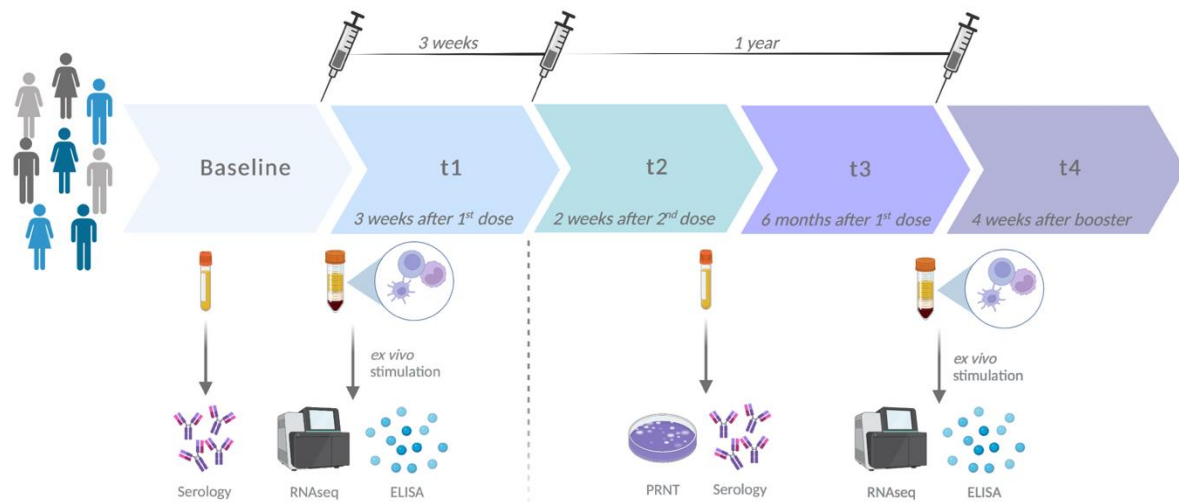
90

91 **Results**

92 **Participants and study design**

93 Sixteen healthcare volunteers who received the BNT162b2 mRNA COVID-19 vaccine as per
94 national vaccination campaign were initially recruited in the study. Participants were 26-59
95 years of age (mean age 39.31 ± 11.3 years), 7 men and 9 women, and without known acute or
96 chronic diseases.

97 Samples were collected at five time points in accordance with the phase 1 trial performed by
98 BioNTech and Pfizer [1]: before vaccination (t0), three weeks after the first dose of 30 μ g of
99 BNT162b2 (t1), two weeks after the second dose (t2) – i.e. 5 weeks after the first dose, six
100 months after the first dose (t3), and four weeks after the booster vaccination, which was
101 approximately one year after the first dose (t4) to obtain a broader view on potential long-term
102 effects of the vaccination. The study design is shown in Fig 1.



103

104 **Fig 1. Study design.** Created with BioRender.com.

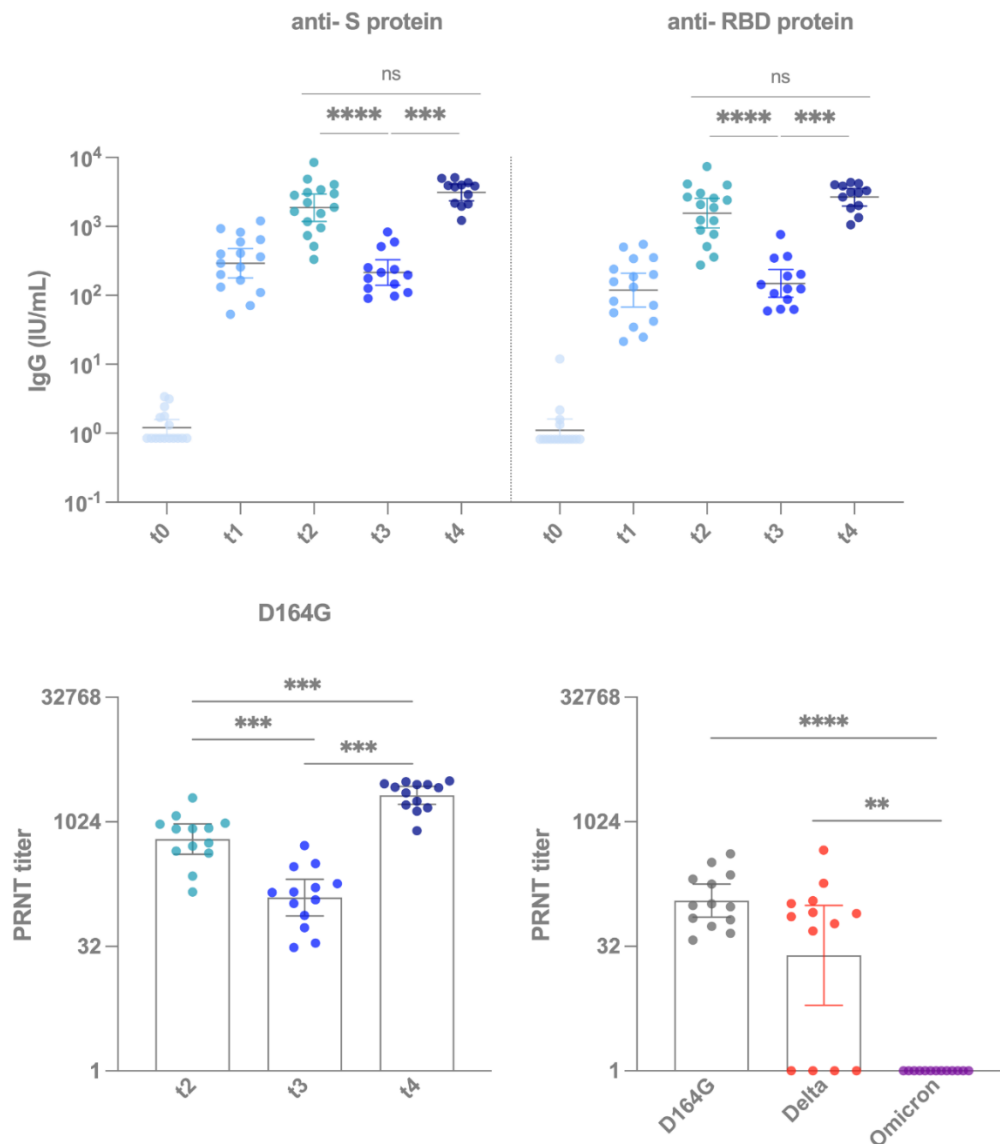
105

106 **Long-term antibody concentrations and neutralization capacity** 107 **against SARS-CoV-2 variants after vaccination with BNT162b2**

108 First, we examined the concentration of receptor-binding domain (RBD)- and spike protein
109 (S)-binding antibody isotype concentrations at given time points (Fig 2a). BNT162b2
110 vaccination elicited high IgG anti-S and anti-RBD concentrations already after the first
111 vaccination and even stronger responses after the second dose of the vaccine. The antibody
112 concentrations significantly decreased six months after vaccination and rose back to the levels
113 of t2 after the booster vaccination.

114 To investigate the neutralizing capacity of the serum against SARS-CoV-2 variants, we
115 performed 50% plaque reduction neutralization testing (PRNT50) using sera collected at t2, t3,
116 and t4 (Fig 2b). After the second dose of BNT162b2, all the serum samples neutralized the
117 D614G strain with titers of at least 1:146, and the geometric mean neutralizing titer (GMT)
118 was 454 IU/ml. Similar to the antibody concentrations, the neutralizing capacity dropped

119 significantly after six months to a GMT of 89 IU/ml. Booster vaccination led to a significant
120 increase in neutralizing titers at t4 (GMT 1533 IU/mL) compared to t2. Finally, we analyzed
121 the neutralizing capacity against different variants at t3. We observed that four of the thirteen
122 samples (31%) failed to neutralize the delta variant, and none were able to neutralize the
123 omicron variant (Fig 2c).



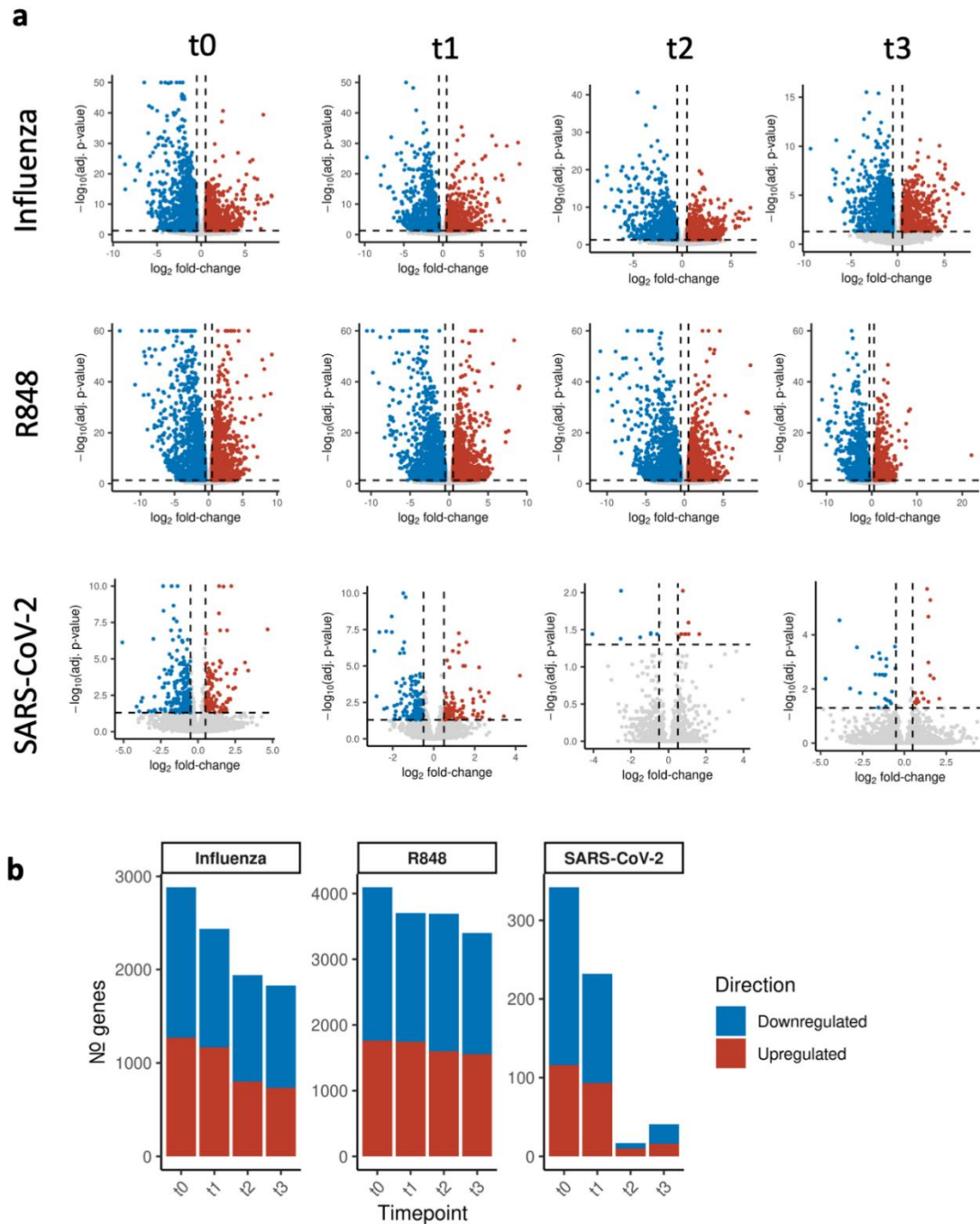
124

125 **Fig 2. BNT162b2 vaccination induced effective antibody responses, but neutralizing capacity**
 126 **started to wane after six months. (a)** S- and RBD-protein specific IgG measured from participants'
 127 plasma collected at t0 (before vaccination), t1 (three weeks after the first dose), t2 (two weeks after the
 128 second dose), t3 (six months after the first dose) and t4 (four weeks after the booster vaccination, which
 129 was approximately one year after the first dose). Wilcoxon test (not corrected for multiple comparisons)
 130 is used to compare different time points. **(b)** PRNT from sera of the participants on Wuhan Hu-1 D164G
 131 after vaccination at depicted time points. Wilcoxon paired test (not corrected for multiple comparisons)
 132 is used to compare two time points to each other. **(c)** PRNT from sera of the participants on different
 133 variants six months after the first dose. Kruskal-Wallis test followed by Dunn's multiple comparison is
 134 used to compare different variants. * p<0.05, ** p<0.01, *** p<0.001, **** p<0.0001. S protein, spike
 135 protein; RBD protein, receptor binding domain protein; IgG, immunoglobuline G; PRNT, plaque
 136 reduction neutralisation test.

137 **Vaccination with BNT162b2 induces long-term transcriptional**
138 **changes in immune cells**

139 We assessed the potential effects of BNT162b2 vaccination on the transcriptional activity of
140 immune cells using bulk RNA sequencing after *ex vivo* stimulation of peripheral blood
141 mononuclear cells (PBMCs) obtained from healthy volunteers before and after vaccination.
142 PBMCs were stimulated with heat-inactivated SARS-CoV-2, as well as with the heterologous
143 stimuli R848, heat-inactivated influenza H1N1 virus or culture medium (RPMI1640; used as
144 an unstimulated control condition).

145 First, we analyzed the responsiveness of the cells by comparing the number of differentially
146 expressed genes (DEGs) induced by specific and non-specific viral stimuli to RPMI treatment
147 within each time point (Figs 3a and 3b). The number of DEGs in PBMCs in response to heat-
148 inactivated influenza, SARS-CoV-2, and R848 stimulation decreased after vaccination
149 compared to RPMI. Especially after the stimulation of PBMCs with SARS-CoV-2, the number
150 of DEGs was substantially lower at the late time points after BNT162b2 immunization. These
151 results show that BNT162b2 vaccination notably affects transcriptional responses to SARS-
152 CoV-2 and heterologous stimuli in PBMCs: interestingly, cells seem to respond less strongly
153 to various stimulations when isolated from volunteers after BNT162b2 vaccination.



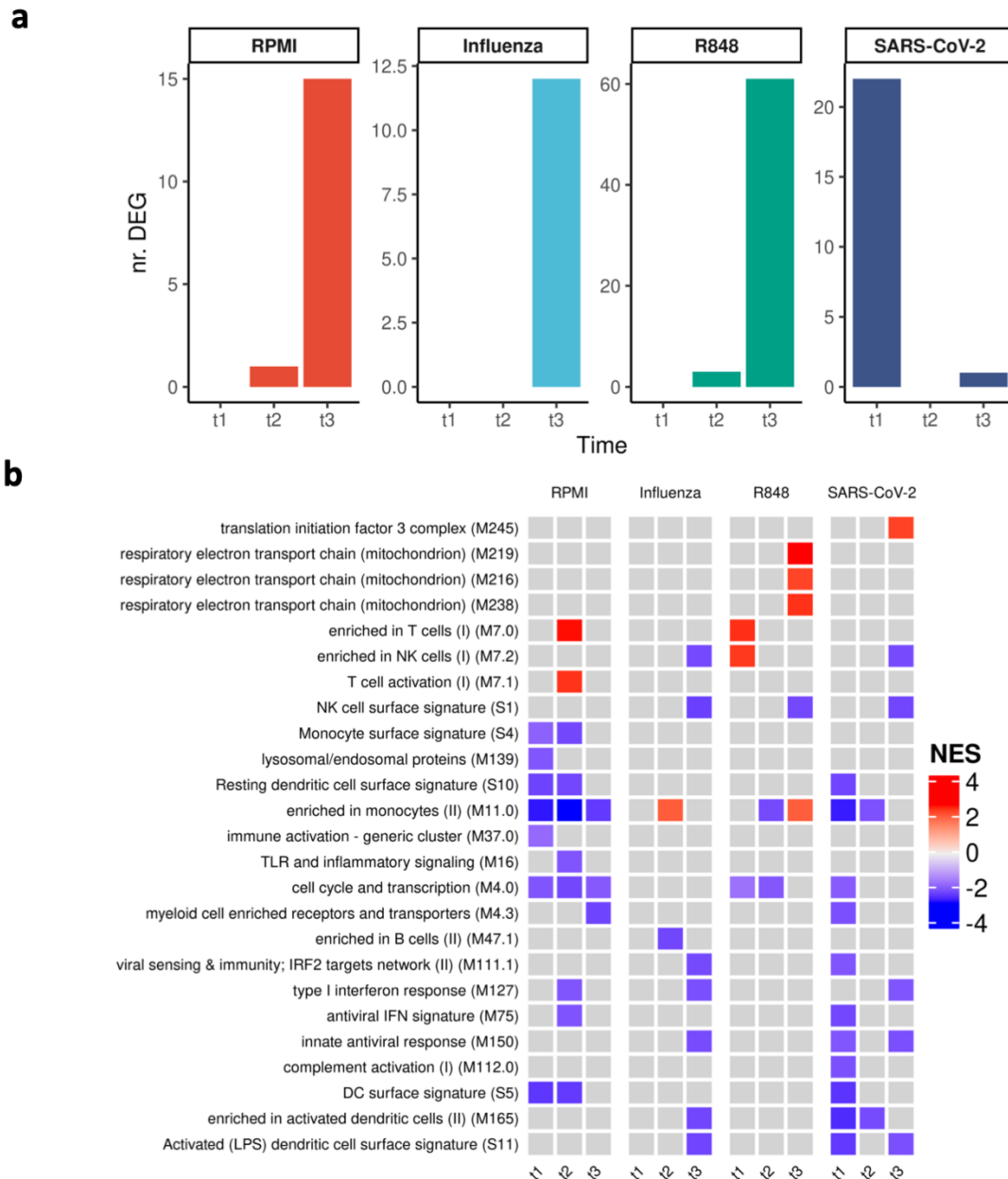
154

155 **Fig 3. Responsiveness to viral stimuli compared to untreated RPMI cells decrease following**
 156 **BNT162b2 vaccination. (a)** Volcano plots presenting the DEGs, showing the log₂-fold-change (x-
 157 axis) vs. the negative log₁₀ of the p-value (y-axis), following the stimulation of the cells (with influenza,
 158 R848 or SARS-CoV-2) and RPMI at t₀ (before vaccination), t₁ (three weeks after the first dose), t₂
 159 (two weeks after the second dose) and t₃ (six months after the first dose). **(b)** Barplot depicting the total
 160 number of DEGs in response to stimulation with influenza, R848 or SARS-CoV-2 compared to RPMI
 161 at t₀, t₁, t₂ and t₃. DEGs, differentially expressed genes.

162 Gene set enrichment was performed to analyze the main cellular processes and pathways
163 affected by the vaccination. Compared to RPMI, chemotaxis pathways were upregulated in all
164 stimulated cells at each time point, whereas the upregulation of T-cell activation and signaling
165 showed a varying pattern (S Fig 1). Interestingly, BNT162b2 vaccination first dampened T cell
166 activation in SARS-CoV-2 stimulated cells, and after six months, the effect reversed.
167 Stimulation with the TLR7/8 agonist R848 induced especially expression of genes related to
168 cell cycle. Conversely, we observed a general downregulation of the gene expression of
169 pathways associated with monocyte and dendritic cell activation. Genes related to (type I) IFN
170 responses and innate antiviral responses were only downregulated following stimulation with
171 influenza, and this was not affected by vaccination. On the contrary, BNT162b2 vaccination
172 induced a persistent downregulation in pathways associated with inflammatory responses,
173 while this effect occurred in the SARS-CoV-2-stimulated cells only after six months.

174 Next, we compared the transcriptional activity of the PBMCs at each time point to pre-
175 vaccination levels within each stimulation to determine if the vaccine induces memory against
176 a particular stimulus (Fig 4a). The number of DEGs in PBMCs incubated with influenza, R848
177 and in RPMI cells increased marginally with each time point, with R848 stimulation showing
178 the most notable change in the numbers. Stimulation with SARS-CoV-2 showed a contrasting
179 pattern with an increased number of DEGs after primary vaccination that returned to baseline
180 levels at the following time points.

181 Gene set enrichment analysis within each stimulus showed downregulation in the type I
182 interferon pathways compared to baseline at t2 and t3 for all stimuli except R848 (Fig 4b).
183 Generally, antiviral immune response-related pathways were downregulated at different points
184 after vaccination. Moreover, genes related to the enrichment of T cells were upregulated in
185 RPMI-treated and R848-stimulated cells after vaccination.



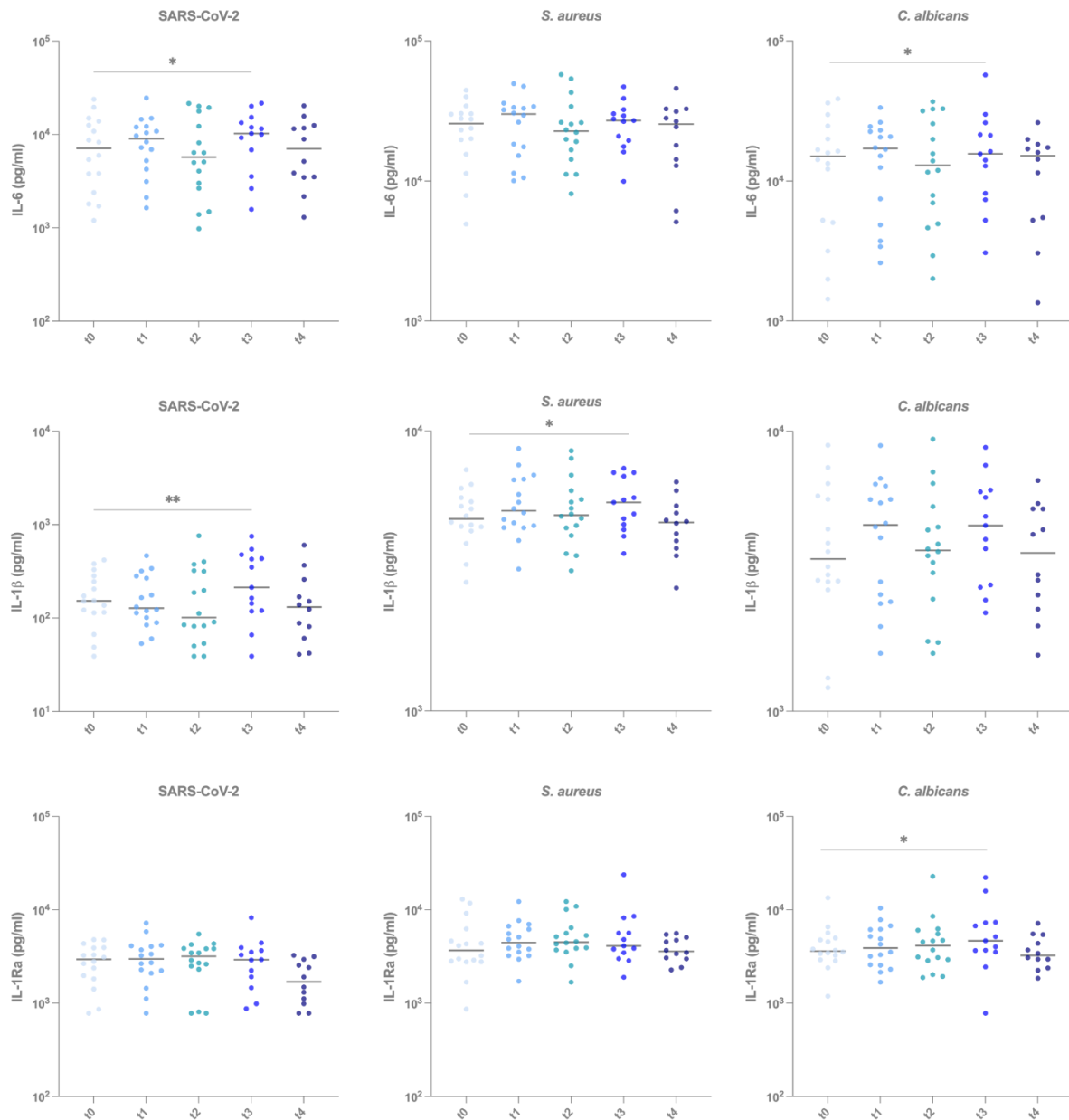
186

187 **Figure 4. DEGs show variation in the course of vaccination and pathways are mostly**
 188 **downregulated compared to the situation before vaccination. (a)** Barplot showing the number of
 189 DEGs of stimulated cells with RPMI, influenza, R848 and SARS-CoV-2 at t1 (three weeks after the
 190 first dose), t2 (two weeks after the second dose) and t3 (six months after the first dose) compared to t0
 191 (before vaccination). **(b)** Heatmap depicting gene set enrichment of cells stimulated with RPMI,
 192 influenza, R848 and SARS-CoV-2 at t1, t2 and t3 to t0. Colors indicate correlation coefficients from
 193 negative (blue) to positive (red). Pathways with $p_{adj} < 0.0001$ are shown. DEGs, differentially
 194 expressed genes.

195

196 **Vaccination with BNT162b2 modifies cytokine production by**
197 **PBMCs in response to different stimuli**

198 In parallel to assessing the transcriptional responses, we measured cytokine secretion by
199 enzyme-linked immunosorbent assay (ELISA) following an *ex vivo* challenge with
200 heterologous stimuli to understand the functional effect of the vaccine on the inflammatory
201 response of PBMCs. To examine the dynamics of cytokine production, we measured IL-6, IL-
202 1 β , TNF- α , and IL-1Ra in response to SARS-CoV-2, the bacterial pathogen *Staphylococcus*
203 *aureus*, and the fungal pathogen *Candida albicans* (Fig 5). IL-6, IL-1 β , and IL-1Ra production
204 capacity varied between time points, but tended to increase six months after the first dose of
205 BNT162b2 compared to baseline. In contrast, the production of TNF- α did not differ before
206 and after the vaccination (S Fig 2).

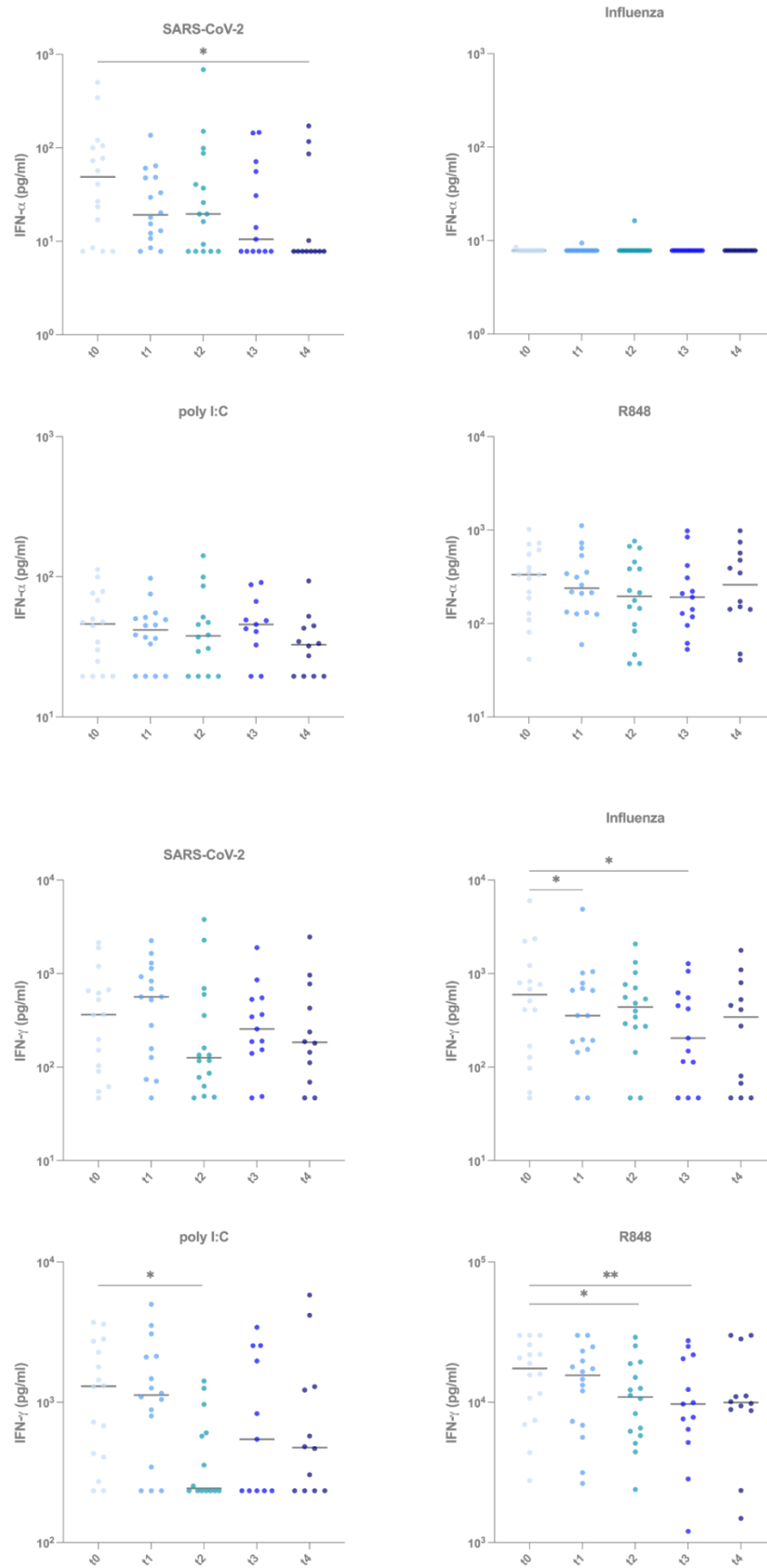


207

208 **Figure 5. Inflammation-related cytokine production against viral, bacterial and fungal stimuli**
 209 **fluctuates through different time points.** IL-6, IL-1β, and IL-1Ra production by human PBMCs
 210 measured by ELISA following 24 hours *ex vivo* stimulation with heat-killed SARS-CoV-2, heat-killed
 211 *S. aureus* and heat-killed *C. albicans* at t0 (before vaccination), t1 (three weeks after the first dose), t2
 212 (two weeks after the second dose), t3 (six months after the first dose) and t4 (four weeks after the booster
 213 vaccination, which was approximately one year after the first dose). Wilcoxon paired test (not corrected
 214 for multiple comparisons) is used to compare the cytokine values measured at different timepoints to
 215 the those of t0 (before vaccination). * p<0.05, ** p<0.01. IL-6, interleukin 6; IL-1β, interleukin 1
 216 beta; IL-1Ra, interleukin-1 receptor antagonist.

217 Interferons are essential for antiviral immunity [10]. Therefore, we measured IFN- α , a type I
218 interferon, in the PBMCs in response to viral stimuli (SARS-CoV-2, influenza, poly I:C, and
219 R848). IFN- α release in response to SARS-CoV-2 decreased over time, with the highest
220 production before the vaccination and the lowest after the booster shot (Fig 6a). We observed
221 a similar drop in the release of IFN- α compared to baseline in response to the TLR3 ligand
222 poly I:C and TLR7/8 ligand R848, potent inducers of IFN- α [11].

223 Subsequently, we measured IFN- γ , a type II interferon produced mainly by NK and T cells,
224 which showed a varying pattern after viral stimulation. There was a decrease in IFN- γ
225 production after the second dose for all stimuli, reaching statistical significance for poly I:C
226 and R848 (Fig 6b). Additionally, the cytokine production continuously dropped with each time
227 point in the case of R848 stimulation. Especially for influenza, we observed a lower production
228 of IFN- γ at t1 and t3 than at baseline.



229

230

15

(Continued)

231 **Figure 6. Type I and type II interferon production after *ex vivo* viral stimulation shows tendency**
232 **to decrease after vaccination. (a)** IFN- α measured by ELISA following 24 hours *ex vivo* stimulation
233 in reponse to heat-killed SARS-CoV-2, heat-killed *S. aureus* and heat-killed *C. albicans* at t0 (before
234 vaccination), t1 (three weeks after the first dose), t2 (two weeks after the second dose), t3 (six months
235 after the first dose) and t4 (four weeks after the booster vaccination, which was approximately one year
236 after the first dose). **(b)** IFN- γ measured by ELISA following 7 days of *ex vivo* stimulation with heat-
237 killed SARS-CoV-2, heat-killed *S. aureus* and heat-killed *C. albicans* at t0, t1, t2, t3 and t4. Wilcoxon
238 paired test (not corrected for multiple comparisons) is used to compare the cytokine values measured at
239 different timepoints to the those of t0 (before vaccination). * p<0.05, ** p<0.01. IFN- α , interferon
240 alpha; IFN- γ , interferon gamma.

241

242 **Discussion**

243 Novel vaccines based on mRNA technology have been recently developed against COVID-19,
244 but much remains to be learned about their wide immunological effects. In this study, we
245 investigated the specific humoral effects of the BNT162b2 vaccine developed by
246 BioNTech/Pfizer, as well as its effects on the innate immune responses to various viral,
247 bacterial, and fungal pathogens. We show that the BNT162b2 vaccine induces long-term
248 effects on both adaptive and innate immune responses, including transcriptional changes and
249 effects on cytokine production capacity.

250 Our findings on the induction of specific anti-SARS-CoV-2 antibodies align with several recent
251 studies. In this respect, we observed a decline in antibody concentrations and neutralizing
252 capacity six months after vaccination [12,13]. It has been hypothesized that this decline is likely
253 caused by plasmablasts that do not differentiate into long-lived memory plasma cells [14].
254 Booster vaccination restored the antibody concentrations, even higher than the concentrations
255 after the first vaccination cycle. However, this increase was not significant, which differs from
256 a few recent reports [15,16]. This discrepancy may be attributed to our reduced sample size, as

257 reports from Salvagno and Teresa Vietri *et al.* have a 3- to 4-fold higher number of individuals
258 included in their studies. In contrast, the neutralizing antibody titers did reach higher levels
259 after the third than after the second vaccination.

260 The lack of neutralizing capacity against the omicron variant after six months underlines the
261 urgent need for booster vaccinations that can target new variants, a finding also reported by
262 others [17,18]. Omicron strains are, at the moment of writing, the most prevalent circulating
263 variants, characterized by large numbers of mutations in the spike protein [19]. Those
264 mutations, together with a recently detected higher affinity for the receptor angiotensin-
265 converting enzyme 2 (ACE2), are suspected to be the reason why omicron variants so
266 effectively escape antibody recognition [20].

267 In the last decade, an increasing number of studies have reported the long-term effects of
268 vaccines not only on adaptive immune responses but also on innate immunity [21]. This results
269 in a *de facto* innate immune memory termed *trained immunity*, which can result in protective
270 effects against heterologous infections [22]. The newly developed COVID-19 vaccines,
271 including those based on mRNA, were shown to have strong inflammatory effects due to their
272 LNP delivery system [4], and we, therefore, set out to assess their potential long-term effect on
273 the induction of trained immunity. First, we assessed the changes in the transcriptional program
274 induced by viral stimulation with inactivated SARS-CoV-2, H1N1 influenza virus, or the
275 TLR7/8 agonist R848 in immune cells after BNT162b2 vaccination. We observed that, after
276 BNT162b2 vaccination, even unstimulated cells (RPMI) showed changes in the number of
277 DEGs. A possible explanation for this might be the inflammatory feature of the LNP-delivered
278 and modified-mRNA components of BNT162b2, as has been pointed out in a mouse model
279 [4]. The multiple downregulated pathways observed following vaccination in unstimulated
280 state may be caused by the exhaustion of the cells under the effects of such an inflammatory

281 stimulus for a long time which mimics chronic infection. It is known that chronic inflammation
282 can result in, for instance, T-cell exhaustion [23].

283 Recently, Arunachalam *et al.* showed that the second BNT162b2 vaccination generated a more
284 pronounced transcriptional response as there was a general increase in the immune
285 responsiveness [5]. However, the authors did not investigate the transcriptional response of
286 immune cells post-vaccination upon viral restimulation. Our data underline the importance of
287 investigating transcriptional responses after a perturbation rather than only in steady-state
288 conditions. On the other hand, we observed increased numbers of DEGs at each consecutive
289 time point in line with the work from Arunachalam *et al.*, except those in SARS-CoV-2
290 stimulated cells, which decreased after secondary vaccination. Additionally, Yamaguchi *et al.*
291 performed ATAC-sequencing of monocytes and observed an initial enhancement of type I IFN-
292 related gene accessibility after the second vaccination, which disappeared after only four weeks
293 [24]. In contrast, our study showed either no change or downregulation in the type I IFN-related
294 pathways, which might suggest that BNT162b2 vaccination induces innate immune memory
295 that also consists of tolerance characteristics.

296 Similar changes in the production of cytokines and interferons accompany the transcriptional
297 responses to viral stimulation after vaccination. In this respect, the production of the cytokines
298 from the IL-1/IL-6 pathway, including the anti-inflammatory IL-1Ra, tended to increase six
299 months after the first vaccination. More remarkable is, however, the tendency of lower
300 interferon responses after BNT162b2 vaccination. BNT162b2 vaccination has been previously
301 reported to activate virus-specific CD4+ and CD8+ T cells and upregulate the production of
302 immune-modulatory cytokines such as IFN- γ shortly after primary and secondary vaccination
303 [5,25–27]. In contrast to these studies, we observed a downregulation of the type I interferon
304 pathway in response to influenza at the transcriptional level, and lower IFN- α production by

305 PBMCs after stimulation with SARS-CoV-2. A similar pattern can be observed for IFN- γ ,
306 which was produced less by PBMCs after immunization when exposed to various viral stimuli.
307 The cause of these different findings is unclear, although using different methodologies may
308 partially explain them. Samanovic et. al., for instance, assessed the percentage of IFN- γ +
309 CD4+, and CD8+ T cells in response to the spike-peptide mix after a relatively short
310 stimulation [25], whereas we measured the secreted cytokine in response to the heat-inactivated
311 virus after a 7-days stimulation period.

312 To understand the heterologous effects of the BNT162b2 vaccine, one should also consider its
313 composition. BNT162b2 comprises N1-methyl-pseudouridine (m1 Ψ) nucleoside-modified
314 mRNA encapsulated in a lipid nanoparticle (LNP) [28]. The pseudouridine modification
315 increases mRNA stability and decreases an anti-RNA immune response [29]. LNPs are chosen
316 as a delivery system for mRNA, which have been first conceptualized decades ago [30–32],
317 and more recently, they have been used to deliver an RNA-based drug (Patisiran®) successfully
318 [33]. Later on, Kariko *et al.* reported that infection of the cells with m1 Ψ nucleoside-modified
319 mRNA could dampen the response through TLR3 and TLR7 [29], which is in line with the
320 results of our study. It could be hypothesized that this is due to the decrease in sensitivity of
321 endosomal TLRs that interact with this transfected modified mRNA, subsequently ablating the
322 activity of TLR3, TLR7, and TLR8 and decreasing cytokine production [34].

323 Another contributing factor in the success of mRNA vaccines was suggested to be the presence
324 of an immunoadjuvant [29,35]. It is known that BNT162b2 does not contain conventional
325 adjuvants; however, LNPs have been shown to act as immunostimulatory adjuvants besides
326 their role in the delivery of the mRNA [35–37]. These findings support the more recent report
327 from Ndeupen et al., showing highly inflammatory characteristics of LNPs in a mouse model
328 [4], which can contribute to the effects of BNT162b2 and other mRNA vaccines.

329 The results of the present study support the hypothesis that BNT162b2 has long-term
330 heterologous effects on immune cells, reminiscent of the induction of trained immunity [22].
331 In a mouse model, Qin et al. showed that mRNA-LNP pre-exposure can alter immune
332 responses to influenza and *C. albicans* infection [6]. These results collectively demonstrate that
333 the effects of the BNT162b2 vaccine go beyond the adaptive immune system and can also
334 modulate innate immune responses. An important question, however, relates to the biological
335 consequences of these effects. Recently, some debate has been ongoing on whether BNT162b2
336 immunization is associated with the reactivation of varicella-zoster virus (VZV) [38]. Possible
337 explanations include the suppression of VZV-specific CD8⁺ cells by the immense shift of naïve
338 CD8⁺ cells after immunization and the downregulation of TLR pathways through
339 immunization and thereby inhibiting of interferon production. The hypothesis of
340 downregulated interferon production agrees with our data, however, the causes of these effect
341 remain to be proven. Our results may explain the data from a recent study of over 50,000
342 healthcare workers that found that the more doses of the mRNA vaccine received by the
343 individuals, the higher their risk of contracting COVID-19 [39]. It may be thus hypothesized
344 that vaccination with mRNA-based vaccines causes dysregulation of innate immune responses,
345 and that the consequences of this effect for protection against SARS-CoV-2 cannot be fully
346 compensated by the induction of adaptive immune responses.

347 On the other hand, the more dampened transcriptional reactivity of the immune cells to
348 secondary viral stimulation (immune tolerance) may provide an explanation for the protective
349 effects of BNT162b2 against severe COVID-19. Overwhelming inflammation is one of the
350 important pathological features in patients with COVID-19. Thus, a more regulated
351 inflammatory response may explain why vaccination had especially effects on the reduction of
352 disease severity in case of the delta and omicron variants, rather than a full protection against
353 infection [40]. Indeed, the complete absence of neutralization capacity against omicron in this

354 and other studies argues that cellular mechanisms, such as other T-cell-mediated or innate
355 immune cell-mediated pathways, are responsible for these effects. Furthermore,
356 downregulation of type I IFN signaling has been suggested to be one of the mechanisms
357 affecting immune memory to SARS-CoV-2 as the generation of long-lived memory cells is
358 dependent on it [41,42].

359 The generalizability of these results is subject to certain limitations. First, the number of
360 volunteers in this study was relatively small, although in line with earlier immunological
361 studies on the effects of COVID-19 vaccines. Second, our cohort consisted of healthcare
362 workers, who are middle-aged and healthy, and future studies on elderly individuals and people
363 with comorbidities and other underlying risk factors for severe COVID-19 infections need to
364 be performed. Third, our study is performed only with individuals with Western European
365 ancestry. Therefore, the conclusions of our study should be tested in populations with different
366 ancestry and alternative lifestyles since the induction of innate and adaptive immune responses
367 is mainly dependent on factors such as genetic background, diet, and exposure to environmental
368 stimuli, which differ between communities around the globe.

369

370 In conclusion, our data show that the BNT162b2 vaccine induces effects on both the adaptive
371 and innate branches of the immune system. Intriguingly, the BNT162b2 vaccine induces
372 significant changes in interferon production, and this needs to be studied in more detail: in
373 combination with strong adaptive immune responses, this could contribute to a more balanced
374 inflammatory reaction during infection with SARS-CoV-2 or other pathogens. Our findings
375 need to be confirmed by conducting larger cohort studies with populations with diverse
376 backgrounds, while further studies should investigate the incidence of heterologous infections
377 after BNT162b2.

378 **Materials and Methods**

379 **Cohort**

380 Healthcare workers from the Radboud University Medical Center, Nijmegen were enrolled
381 who received the BNT162b2 mRNA COVID-19 vaccine as per national vaccination campaign
382 and provided informed consent. Key exclusion criteria included a medical history of COVID-
383 19. Participants were asked at each study visit whether they had COVID-19 since the previous
384 study visit. One individual was removed from the dataset after detecting high concentrations
385 of antibodies against SARS-CoV-2 N-antigen at baseline and two individuals were removed at
386 later time points because they had COVID-19 in the course of the study.

387

388 **Virus isolation and sequencing**

389 Viruses were isolated from diagnostic specimen at the department of Viroscience, Erasmus
390 MC, and subsequently sequenced to rule out additional mutations in the S protein. SARS-CoV-
391 2 isolate BetaCoV/Munich/BavPat1/2020 (European Virus Archive 026V-03883), was kindly
392 provided by Prof. C. Drosten. At 72 h post-infection, the culture supernatant was centrifuged
393 for 5 min at 1500 x g and filtered through an 0.45 µm low protein binding filter (Sigma-Aldrich,
394 Germany, cat #SLHPR33RS). To further purify the viral stocks, the medium was transferred
395 over an Amicon Ultra-15 column with 100 kDa cutoff (Sigma-Aldrich, Germany, cat
396 #UFC910008), which was washed 3 times using Opti-MEM supplemented with GlutaMAX
397 (Thermo Fisher Scientific, USA, cat #51985034). Afterwards, the concentrated virus on the
398 filter was diluted back to the original volume using Opti-MEM, and the purified viral aliquots
399 were stored at -80 °C. The infectious viral titers were measured using plaque assays as

400 described [43] and stocks were heat inactivated for 60 min at 56 °C for use in stimulation
401 experiments.

402

403 **Measurement of antibody concentrations against RBD and Spike** 404 **protein**

405 For antibody analysis, a fluorescent-bead-based multiplex immunoassay (MIA) was
406 developed, as previously described by Fröberg et al., 2021, with some slight modifications
407 [44]. The first international standard for anti-SARS-CoV-2 immunoglobulin, (20/136, NIBSC),
408 was used to create standard curves. Next to this, four different samples from PCR-confirmed
409 COVID-19 patients were used as quality control samples. Serum samples were diluted 1:500
410 and 1:8000 in assay buffer (SM01/1%BSA), and incubated with antigen-coated microspheres
411 for 45 min at room temperature while shaking at 450 rpm. Purified S (Stabilized Trimeric Spike
412 Protein from the Wuhan variant) and receptor binding domain (RBD from the Wuhan variant)
413 proteins purchased from ExcellGene were coupled to microspheres. Following incubation with
414 sera, the microspheres were washed three times with PBS/0,05% Tween-20, incubated with
415 phycoerythrin-conjugated goat anti-human, IgG (Jackson ImmunoResearch, 109-116-170) for
416 20 min and washed three times. Data were acquired on the Luminex FlexMap3D System.
417 Validation of the detection antibodies was obtained from a recent publication using the same
418 antibodies and the same assay [45], and specificity was checked using rabbit anti-SARS SIA-
419 ST serum. MFI was converted to International Units (IU/ml) by interpolation from a log-5PL-
420 parameter logistic standard curve and log-log axis transformation using Bioplex Manager 6.2
421 (Bio-Rad Laboratories) software and exported to R-studio.

422 **Plaque reduction neutralization assay**

423 A plaque reduction neutralization test (PRNT) was performed. Viruses used in the assay were
424 isolated from diagnostic specimen at the department of Viroscience, Erasmus MC, cultured
425 and subsequently sequenced to rule out additional mutations in the S protein. Heat-inactivated
426 sera were 2-fold diluted in Dulbecco modified Eagle medium supplemented with NaHCO₃,
427 HEPES buffer, penicillin, streptomycin, and 1% fetal bovine serum, starting at a dilution of
428 1:10 in 60 µL. We then added 60 µL of virus suspension (400 plaque-forming units) to each
429 well and incubated at 37 °C for 1h. After 1 hour incubation, we transferred the mixtures on to
430 Vero-E6 cells and incubated for 8 hours. After incubation, we fixed the cells with 10%
431 formaldehyde and stained the cells with polyclonal rabbit anti-SARS-CoV antibody (Sino
432 Biological) and a secondary peroxidase-labeled goat anti-rabbit IgG (Dako). We developed
433 signal by using a precipitate forming 3,3',5,5'-tetramethylbenzidine substrate (True Blue;
434 Kirkegaard and Perry Laboratories) and counted the number of infected cells per well by using
435 an ImmunoSpot Image Analyzer (CTL Europe GmbH). The serum neutralization titer is the
436 reciprocal of the highest dilution resulting in an infection reduction of >50% (PRNT50). We
437 considered a titer >20 to be positive based on assay validation.

438

439 **Isolation of peripheral blood mononuclear cells**

440 Blood samples from participants were collected into EDTA-coated tubes (BD Bioscience,
441 USA) and used as the source of peripheral blood mononuclear cells (PBMCs) after sampling
442 sera from each individual. Blood was diluted 1:1 with PBS (1X) without Ca⁺⁺, Mg⁺⁺
443 (Westburg, The Netherlands, cat #LO BE17-516F) and PBMCs were isolated via density
444 gradient centrifuge using Ficoll-PaqueTM-plus (VWR, The Netherlands, cat #17-1440-03P).

445 Specialized SepMate-50 tubes were used for the isolation (Stem Cell Technologies, cat
446 #85450). Cells counts were determined via Sysmex XN-450 (Japan) hematology analyzer.
447 Afterwards, PBMCs were frozen using Recovery Cell Culture Freezing Medium (Thermo
448 Fisher Scientific, USA, cat #12648010) in the concentration of 15×10^6 /mL.

449

450 **Stimulation experiments**

451 The PBMCs were thawed and washed with 10mL Dutch modified RPMI 1640 medium
452 (Roswell Park Memorial Institute; Invitrogen, USA, cat # 22409031) containing 50 μ g/mL
453 Gentamicine (Centrafarm, The Netherlands), 1 mM Sodium-Pyruvate (Thermo Fisher
454 Scientific, USA, cat #11360088), 2 mM Glutamax (Thermo Fisher Scientific, USA, cat
455 #35050087) supplemented with 10% Bovine Calf Serum (Fisher Scientific, USA, cat
456 #11551831) twice. DNase (Roche, Switzerland, cat #1128493200) was added to the wash
457 medium to digest extracellular DNA released from dying cells. Afterwards, the cells were
458 counted via Sysmex XN-450. PBMCs (4×10^5 cells/well) stimulated in sterile round bottom 96-
459 well tissue culture treated plates (VWR, The Netherlands, cat #734-2184) in Dutch modified
460 RPMI 1640 medium containing 50 μ g/mL Gentamicine, 1 mM Sodium-Pyruvate, 2 mM
461 Glutamax supplemented with 10% human pooled serum. Stimulations were done with heat-
462 inactivated SARS-CoV-2, Wuhan Hu-1 (GISAID accession number is EPI_ISL_425126,
463 Wuhan-Hu-1 WT [46], (2.8×10^3 TCID₅₀/mL), influenza virus reference strain
464 A/California/7/2009 H1N1 was used (described in [47]) (3.6×10^3 TCID₅₀/mL), 10 μ g/mL Poly
465 I:C (Invivogen, USA, cat #tlrl-pic), 3 μ g/mL R848 (Invivogen, USA, cat #tlrl-r848), 1 x
466 10^6 /mL *S. aureus* and 1 x 10^6 /mL *C. albicans*. The PBMCs were incubated with the stimulants
467 for 24 hours to detect IL-1 β , TNF- α , IL-6, IL-1Ra and IFN- α , and 7 days to detect IFN- γ as
468 well as bulk RNA isolation. Supernatants were collected and stored in -20 °C. Secreted

469 cytokine levels from supernatants were quantified by ELISA (IL-1 β cat # DLB50, TNF- α cat
470 # STA00D, IL-6 cat # D6050, IL-1Ra cat # DRA00B, IFN- γ cat #DY285B, R&D Systems,
471 USA and IFN- α cat #3425-1H-20, Mabtech, Sweden) following manufacturers' instructions.

472

473 **Bulk RNAseq analysis**

474 Bulk RNA sequencing data were processed using the publicly available nfcore/rnaseq pipeline
475 (v2.0, [48]), implemented in Nextflow (v21.04.3, [49]) using default settings. Reads were
476 aligned to the human GRCh38 genome.

477 Further downstream analyses were performed in R (v4.2.0, [50]) using DESeq2 (v1.36, [51]).

478 Manual curation of quality control metrics and principal component analysis (PCA) was

479 performed per timepoint and stimulation separately to identify potential outliers. 13 out of 242

480 samples were removed from further analysis.

481

482 **Statistical analysis**

483 Graphpad Prism 8 was used for all statistical analyses. Outcomes between paired groups were

484 analyzed by Wilcoxon's matched-pairs signed-rank test (not corrected for multiple

485 comparisons). Three or more groups were compared using Kruskal-Wallis Test - Dunnet's

486 multiple comparison. A p-value of less than 0.05 was considered statistically significant (*

487 $p < 0.05$, ** $p < 0.01$, *** $p < 0.001$, **** $p < 0.0001$). Spearman correlation was used to determine

488 correlation between groups.

489 For bulk RNA sequencing, differential gene expression was estimated using linear models that

490 included individual's sex and their age class (<40 or >40 years of age). Genes with total read

491 counts < 20 were removed prior to this analysis. Resulting p-values were corrected across all

492 genes using Benjamini-Hochberg. Genes with adjusted p-values < 0.05 and $\log_{2}FC > 0.5$ were
493 considered significantly differentially expressed. For gene set enrichment analysis, we used
494 blood transcription modules [52]. Genes were ranked by the Wald statistic and p-values were
495 adjusted using Benjamini-Hochberg. Adjusted P-values < 0.05 were considered significant.
496

497 **Study approval**

498 The study was approved by the Arnhem-Nijmegen Institutional Review Board (protocol
499 NL76421.091.21) and registered in the EU clinical trials register (EudraCT: 2021-000182-33).
500

501 **Data and code availability**

502 The RNAseq datasets generated during and/or analyzed during the current study are included
503 as electronic supplementary material. The other data is available upon request.
504

505 **Acknowledgements**

506 We thank all the volunteers to the study for their willingness to participate and the research
507 technicians (Helga Dijkstra, Heidi Lemmers, S. Andrei Sarlea and Maartje Reijnders) for their
508 help in collecting samples.
509

510 **Declaration of Interests**

511 M.G.N and L.A.B.J are scientific founders of TTxD and Lemba.

512 **Funding**

513 L.A.B.J. is supported by a Competitiveness Operational Program Grant of the Romanian
514 Ministry of European Funds (HINT, ID P_37_762; MySMIS 103587). J.D-A. is supported by
515 the Netherlands Organization for Scientific Research (VENI grant 09150161910024 and Off-
516 Road grant 04510012010022). M.G.N. is supported by an ERC Advanced Grant (#833247)
517 and a Spinoza Grant of the Netherlands Organization for Scientific Research.

518 **References**

- 519 1. Walsh E, Frenck R, Falsey A, et al. Safety and immunogenicity of two RNA-based
520 Covid-19 vaccine candidates. *New Eng J Med* **2020**; 383:2439–2450.
- 521 2. Polack FP, Thomas SJ, Kitchin N, et al. Safety and Efficacy of the BNT162b2 mRNA
522 Covid-19 Vaccine. *New England Journal of Medicine* **2020**; 383:2603–2615.
- 523 3. Sahin U, Muik A, Derhovanessian E, et al. COVID-19 vaccine BNT162b1 elicits
524 human antibody and TH1 T cell responses. *Nature* **2020**;
- 525 4. Ndeupen S, Qin Z, Jacobsen S, Bouteau A, Estanbouli H, Igyártó BZ. The mRNA-
526 LNP platform’s lipid nanoparticle component used in preclinical vaccine studies is
527 highly inflammatory. *iScience* **2021**; 24:103479. Available at:
528 <http://www.cell.com/article/S2589004221014504/fulltext>. Accessed 26 September
529 2022.
- 530 5. Arunachalam PS, D Scott MK, Hagan T, et al. Systems vaccinology of the BNT162b2
531 mRNA vaccine in humans. *410 | Nature |* **2021**; 596. Available at:
532 <https://doi.org/10.1038/s41586-021-03791-x>.
- 533 6. Qin Z, Lie Bouteau A, Herbst C, Igyá Rtó Id BZ. Pre-exposure to mRNA-LNP inhibits
534 adaptive immune responses and alters innate immune fitness in an inheritable fashion.
535 *PLoS Pathog* **2022**; 18:e1010830. Available at:
536 <https://journals.plos.org/plospathogens/article?id=10.1371/journal.ppat.1010830>.
537 Accessed 26 September 2022.
- 538 7. Kleinnijenhuis J, Quintin J, Preijers F, et al. Bacille Calmette-Guerin induces NOD2-
539 dependent nonspecific protection from reinfection via epigenetic reprogramming of
540 monocytes. *Proc Natl Acad Sci U S A* **2012**; 109:17537–17542.
- 541 8. Wimmers F, Donato M, Kuo A, et al. The single-cell epigenomic and transcriptional
542 landscape of immunity to influenza vaccination. *Cell* **2021**; 184:3915-3935.e21.
- 543 9. Murphy DM, Cox DJ, Connolly SA, et al. Trained immunity is induced in humans
544 after immunization with an adenoviral vector COVID-19 vaccine. *J Clin Invest* **2022**;
- 545 10. Hadjadj J, Yatim N, Barnabei L, et al. Impaired type I interferon activity and
546 inflammatory responses in severe COVID-19 patients. *Science (1979)* **2020**; 369:718–
547 724. Available at: <http://science.sciencemag.org/>. Accessed 2 May 2021.
- 548 11. Smith N, Possémé C, Bondet V, et al. Defective activation and regulation of type I
549 interferon immunity is associated with increasing COVID-19 severity. *Nature*

- 550 Communications 2022 13:1 **2022**; 13:1–14. Available at:
551 <https://www.nature.com/articles/s41467-022-34895-1>. Accessed 22 December 2022.
- 552 12. Gandolfo C, Anichini G, Mugnaini M, et al. Overview of Anti-SARS-CoV-2 Immune
553 Response Six Months after BNT162b2 mRNA Vaccine. *Vaccines* 2022, Vol 10, Page
554 171 **2022**; 10:171. Available at: <https://www.mdpi.com/2076-393X/10/2/171/htm>.
555 Accessed 28 September 2022.
- 556 13. Levin EG, Lustig Y, Cohen C, et al. Waning Immune Humoral Response to
557 BNT162b2 Covid-19 Vaccine over 6 Months. *New England Journal of Medicine* **2021**;
558 385:e84. Available at: <https://www.nejm.org/doi/full/10.1056/nejmoa2114583>.
559 Accessed 28 September 2022.
- 560 14. Cohen KW, Linderman SL, Moodie Z, et al. Longitudinal analysis shows durable and
561 broad immune memory after SARS-CoV-2 infection with persisting antibody
562 responses and memory B and T cells. *Cell Rep Med* **2021**; 2:100354.
- 563 15. Salvagno GL, Henry BM, Pighi L, de Nitto S, Gianfilippi G, Lippi G. Effect of
564 BNT162b2 booster dose on anti-SARS-CoV-2 spike trimeric IgG antibodies in
565 seronegative individuals. *Clin Chem Lab Med* **2022**; 60:930–933. Available at:
566 <https://pubmed.ncbi.nlm.nih.gov/35303764/>. Accessed 28 September 2022.
- 567 16. Teresa Vietri M, D’Elia G, Caliendo G, et al. Antibody levels after BNT162b2 vaccine
568 booster and SARS-CoV-2 Omicron infection. *Vaccine* **2022**; 40. Available at:
569 <https://pubmed.ncbi.nlm.nih.gov/36041940/>. Accessed 28 September 2022.
- 570 17. Edara VV, Manning KE, Ellis M, et al. mRNA-1273 and BNT162b2 mRNA vaccines
571 have reduced neutralizing activity against the SARS-CoV-2 omicron variant. *Cell Rep*
572 *Med* **2022**; 3. Available at: <https://pubmed.ncbi.nlm.nih.gov/35233550/>. Accessed 28
573 September 2022.
- 574 18. GeurtsvanKessel CH, Geers D, Schmitz KS, et al. Divergent SARS-CoV-2 Omicron-
575 reactive T and B cell responses in COVID-19 vaccine recipients. *Sci Immunol* **2022**;
576 7:eabo2202. Available at: <https://www.science.org/doi/10.1126/sciimmunol.abo2202>.
577 Accessed 28 September 2022.
- 578 19. Tian D, Sun Y, Xu H, Ye Q. The emergence and epidemic characteristics of the highly
579 mutated SARS-CoV-2 Omicron variant. *J Med Virol* **2022**; 94:2376–2383. Available
580 at: <https://pubmed.ncbi.nlm.nih.gov/35118687/>. Accessed 22 December 2022.
- 581 20. Shah M, Woo HG. Omicron: A Heavily Mutated SARS-CoV-2 Variant Exhibits
582 Stronger Binding to ACE2 and Potently Escapes Approved COVID-19 Therapeutic
583 Antibodies. *Front Immunol* **2022**; 12:6031.

- 584 21. Geckin B, Föhse FK, Domínguez-Andrés J, Netea MG. Trained immunity:
585 implications for vaccination. *Curr Opin Immunol* **2022**; 77:102190.
- 586 22. Netea MG, Domínguez-Andrés J, Barreiro LB, et al. Defining trained immunity and its
587 role in health and disease. *Nat Rev Immunol*. 2020;
- 588 23. Wherry EJ, Kurachi M. Molecular and cellular insights into T cell exhaustion. *Nature*
589 *Reviews Immunology* 2015 15:8 **2015**; 15:486–499. Available at:
590 <https://www.nature.com/articles/nri3862>. Accessed 22 December 2022.
- 591 24. Yamaguchi Y, Kato Y, Edahiro R, et al. Consecutive BNT162b2 mRNA vaccination
592 induces short-term epigenetic memory in innate immune cells. *JCI Insight* **2022**;
- 593 25. Samanovic MI, Cornelius AR, Gray-Gaillard SL, et al. Robust immune responses are
594 observed after one dose of BNT162b2 mRNA vaccine dose in SARS-CoV-2-
595 experienced individuals. *Sci Transl Med* **2022**; 14:8961. Available at:
596 <https://www.science.org/doi/10.1126/scitranslmed.abi8961>. Accessed 26 September
597 2022.
- 598 26. Bergamaschi C, Terpos E, Rosati M, et al. Systemic IL-15, IFN- γ , and IP-10/CXCL10
599 signature associated with effective immune response to SARS-CoV-2 in BNT162b2
600 mRNA vaccine recipients. *Cell Rep* **2021**; 36. Available at:
601 <https://pubmed.ncbi.nlm.nih.gov/34352226/>. Accessed 28 September 2022.
- 602 27. Li C, Lee A, Grigoryan L, et al. Mechanisms of innate and adaptive immunity to the
603 Pfizer-BioNTech BNT162b2 vaccine. *Nature Immunology* 2022 23:4 **2022**; 23:543–
604 555. Available at: <https://www.nature.com/articles/s41590-022-01163-9>. Accessed 26
605 September 2022.
- 606 28. Pulendran B, S. Arunachalam P, O’Hagan DT. Emerging concepts in the science of
607 vaccine adjuvants. *Nature Reviews Drug Discovery* 2021 20:6 **2021**; 20:454–475.
608 Available at: <https://www.nature.com/articles/s41573-021-00163-y>. Accessed 14
609 October 2021.
- 610 29. Karikó K, Muramatsu H, Welsh FA, et al. Incorporation of Pseudouridine Into mRNA
611 Yields Superior Nonimmunogenic Vector With Increased Translational Capacity and
612 Biological Stability. *Molecular Therapy* **2008**; 16:1833–1840.
- 613 30. Dimitriadis GJ. Translation of rabbit globin mRNA introduced by liposomes into
614 mouse lymphocytes. *Nature* **1978**; 274:923–924. Available at:
615 <https://pubmed.ncbi.nlm.nih.gov/683336/>. Accessed 26 September 2022.

- 616 31. Malone RW, Felgner PL, Verma IM. Cationic liposome-mediated RNA transfection.
617 Proc Natl Acad Sci U S A **1989**; 86:6077–6081. Available at:
618 <https://pubmed.ncbi.nlm.nih.gov/2762315/>. Accessed 26 September 2022.
- 619 32. Ostro MJ, Giacomoni D, Lavelle D, Paxton W, Dray S. Evidence for translation of
620 rabbit globin mRNA after liposome-mediated insertion into a human cell line. Nature
621 **1978**; 274:921–923. Available at: <https://pubmed.ncbi.nlm.nih.gov/683335/>. Accessed
622 26 September 2022.
- 623 33. Hoy SM. Patisiran: First Global Approval. Drugs **2018**; 78:1625–1631. Available at:
624 <https://pubmed.ncbi.nlm.nih.gov/30251172/>. Accessed 28 September 2022.
- 625 34. Karikó K, Buckstein M, Ni H, Weissman D. Suppression of RNA recognition by Toll-
626 like receptors: The impact of nucleoside modification and the evolutionary origin of
627 RNA. Immunity **2005**; 23:165–175. Available at:
628 <http://www.cell.com/article/S1074761305002116/fulltext>. Accessed 26 September
629 2022.
- 630 35. Alfagih IM, Aldosari B, Alquadeib B, Almurshedi A, Alfagih MM. Nanoparticles as
631 Adjuvants and Nanodelivery Systems for mRNA-Based Vaccines. Pharmaceutics
632 **2020**; 13:1–27. Available at: <https://pubmed.ncbi.nlm.nih.gov/33396817/>. Accessed 26
633 September 2022.
- 634 36. Kedmi R, Ben-Arie N, Peer D. The systemic toxicity of positively charged lipid
635 nanoparticles and the role of Toll-like receptor 4 in immune activation. Biomaterials
636 **2010**; 31:6867–6875.
- 637 37. Wadhwa A, Aljabbari A, Lokras A, Foged C, Thakur A. Opportunities and Challenges
638 in the Delivery of mRNA-Based Vaccines. Pharmaceutics 2020, Vol 12, Page 102
639 **2020**; 12:102. Available at: <https://www.mdpi.com/1999-4923/12/2/102/htm>.
640 Accessed 26 September 2022.
- 641 38. Triantafyllidis KK, Giannos P, Mian IT, Kyrtsionis G, Kechagias KS. Varicella Zoster
642 Virus Reactivation Following COVID-19 Vaccination: A Systematic Review of Case
643 Reports. Vaccines (Basel) **2021**; 9. Available at:
644 <https://pubmed.ncbi.nlm.nih.gov/34579250/>. Accessed 22 December 2022.
- 645 39. Shrestha NK, Burke PC, Nowacki AS, Simon JF, Hagen A, Gordon SM. Effectiveness
646 of the Coronavirus Disease 2019 (COVID-19) Bivalent Vaccine. medRxiv
647 **2022**; :2022.12.17.22283625. Available at:
648 <https://www.medrxiv.org/content/10.1101/2022.12.17.22283625v1>. Accessed 23
649 January 2023.

- 650 40. Bar-On YM, Goldberg Y, Mandel M, et al. Protection by a Fourth Dose of BNT162b2
651 against Omicron in Israel. *New England Journal of Medicine* **2022**; 386:1712–1720.
652 Available at: <https://www.nejm.org/doi/full/10.1056/NEJMoa2201570>. Accessed 22
653 December 2022.
- 654 41. Moga E, Lynton-Pons E, Domingo P. The Robustness of Cellular Immunity
655 Determines the Fate of SARS-CoV-2 Infection. *Front Immunol* **2022**; 13:3170.
- 656 42. Kolumam GA, Thomas S, Thompson LJ, Sprent J, Murali-Krishna K. Type I
657 interferons act directly on CD8 T cells to allow clonal expansion and memory
658 formation in response to viral infection. *Journal of Experimental Medicine* **2005**;
659 202:637–650. Available at: www.jem.org/cgi/doi/10.1084/jem.20050821. Accessed 22
660 December 2022.
- 661 43. Varghese FS, van Woudenberg E, Overheul GJ, et al. Berberine and Obatoclox
662 Inhibit SARS-Cov-2 Replication in Primary Human Nasal Epithelial Cells In Vitro.
663 *Viruses* 2021, Vol 13, Page 282 **2021**; 13:282. Available at:
664 <https://www.mdpi.com/1999-4915/13/2/282/htm>. Accessed 20 January 2023.
- 665 44. Fröberg J, Gillard J, Philipsen R, et al. SARS-CoV-2 mucosal antibody development
666 and persistence and their relation to viral load and COVID-19 symptoms. *Nature*
667 *Communications* 2021 12:1 **2021**; 12:1–11. Available at:
668 <https://www.nature.com/articles/s41467-021-25949-x>. Accessed 4 January 2023.
- 669 45. den Hartog G, Schepp RM, Kuijper M, et al. SARS-CoV-2–Specific Antibody
670 Detection for Seroepidemiology: A Multiplex Analysis Approach Accounting for
671 Accurate Seroprevalence. *J Infect Dis* **2020**; 222:1452. Available at:
672 [/pmc/articles/PMC7454740/](https://pubmed.ncbi.nlm.nih.gov/32444440/). Accessed 4 January 2023.
- 673 46. Ramani A, Müller L, Ostermann PN, et al. SARS-CoV-2 targets neurons of 3D human
674 brain organoids. *EMBO J* **2020**; 39:e106230. Available at:
675 <https://onlinelibrary.wiley.com/doi/full/10.15252/embj.2020106230>. Accessed 22
676 December 2022.
- 677 47. Grund S, Adams O, Wählisch S, Schweiger B. Comparison of hemagglutination
678 inhibition assay, an ELISA-based micro-neutralization assay and colorimetric
679 microneutralization assay to detect antibody responses to vaccination against influenza
680 A H1N1 2009 virus. *J Virol Methods* **2011**; 171:369–373. Available at:
681 <https://pubmed.ncbi.nlm.nih.gov/21146560/>. Accessed 22 December 2022.
- 682 48. Ewels PA, Peltzer A, Fillinger S, et al. The nf-core framework for community-curated
683 bioinformatics pipelines. *Nature Biotechnology* 2020 38:3 **2020**; 38:276–278.

- 684 Available at: <https://www.nature.com/articles/s41587-020-0439-x>. Accessed 20
685 November 2022.
- 686 49. di Tommaso P, Chatzou M, Floden EW, Barja PP, Palumbo E, Notredame C.
687 Nextflow enables reproducible computational workflows. *Nature Biotechnology* 2017
688 35:4 **2017**; 35:316–319. Available at: <https://www.nature.com/articles/nbt.3820>.
689 Accessed 20 November 2022.
- 690 50. R: The R Project for Statistical Computing. Available at: [https://www.r-](https://www.r-project.org/index.html)
691 [project.org/index.html](https://www.r-project.org/index.html). Accessed 22 December 2022.
- 692 51. Love MI, Huber W, Anders S. Moderated estimation of fold change and dispersion for
693 RNA-seq data with DESeq2. *Genome Biol* **2014**; 15:1–21. Available at:
694 <https://genomebiology.biomedcentral.com/articles/10.1186/s13059-014-0550-8>.
695 Accessed 20 November 2022.
- 696 52. Li S, Roupheal N, Duraisingham S, et al. Molecular signatures of antibody responses
697 derived from a systems biology study of five human vaccines. *Nat Immunol* **2014**;
698 15:195–204. Available at: <https://pubmed.ncbi.nlm.nih.gov/24336226/>. Accessed 22
699 December 2022.

700